Cellular Signalling 104 (2023) 110587

Contents lists available at ScienceDirect

Cellular Signalling

journal homepage: www.elsevier.com/locate/cellsig

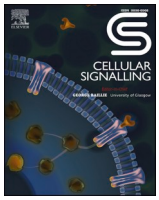

Early adipogenesis is repressed through the newly identified FHL2-NFAT5 signaling complex

Maria P. Clemente-Olivo [a,b,1], Miguel Hernández-Quiles [c,1], Rinske Sparrius [a], Miesje M. van der Stoel [a,2], Vera Janssen [a], Jayron J. Habibe [a,b], Janny van den Burg [a], Aldo Jongejan [d], Paula Alcaraz-Sobrevals [e], Robert van Es [e], Harmjan Vos [e], Eric Kalkhoven [c,3], Carlie J.M. de Vries [a,b,*,3]

[a] Amsterdam UMC location University of Amsterdam, Department of Medical Biochemistry, Amsterdam, the Netherlands
[b] Amsterdam Cardiovascular Sciences, and Amsterdam Gastroenterology, Endocrinology and Metabolism, University of Amsterdam, Amsterdam, the Netherlands
[c] Center for Molecular Medicine, University Medical Center Utrecht, Utrecht University, Utrecht, the Netherlands
[d] Amsterdam UMC location University of Amsterdam, Department of Bioinformatics, Amsterdam, the Netherlands
[e] Oncode Institute and Molecular Cancer Research, Center for Molecular Medicine, University Medical Center Utrecht, Utrecht University, Utrecht, the Netherlands

ARTICLE INFO

Keywords:
Mesenchymal stem cell
FHL2
NFAT5
Adipogenesis
Aging

ABSTRACT

The LIM-domain-only protein FHL2 is a modulator of signal transduction and has been shown to direct the differentiation of mesenchymal stem cells towards osteoblast and myocyte phenotypes. We hypothesized that FHL2 may simultaneously interfere with the induction of the adipocyte lineage. Therefore, we investigated the role of FHL2 in adipocyte differentiation. For these studies pre-adipocytes isolated from mouse adipose tissue and the 3T3-L1 (pre)adipocyte cell line were applied. We performed FHL2 gain of function and knockdown experiments followed by extensive RNAseq analyses and phenotypic characterization of the cells by oil-red O (ORO) lipid staining. Through affinity-purification mass spectrometry (AP-MS) novel FHL2 interacting proteins were identified. Here we report that FHL2 is expressed in pre-adipocytes and for accurate adipocyte differentiation, this protein needs to be downregulated during the early stages of adipogenesis. More specifically, constitutive overexpression of FHL2 drastically inhibits adipocyte differentiation in 3T3-L1 cells, which was demonstrated by suppressed activation of the adipogenic gene expression program as shown by RNAseq analyses, and diminished lipid accumulation. Analysis of the protein-protein interactions mediating this repressive activity of FHL2 on adipogenesis revealed the interaction of FHL2 with the Nuclear factor of activated T-cells 5 (NFAT5). NFAT5 is an established inhibitor of adipocyte differentiation and its knockdown rescued the inhibitory effect of FHL2 overexpression on 3T3-L1 differentiation, indicating that these proteins act cooperatively. We present a new regulatory function of FHL2 in early adipocyte differentiation and revealed that FHL2-mediated inhibition of pre-adipocyte differentiation is dependent on its interaction with NFAT5. FHL2 expression increases with aging, which may affect mesenchymal stem cell differentiation, more specifically inhibit adipocyte differentiation.

Abbreviation: ADIPOQ, adiponectin; CFD, Adipsin; AP-MS, Affinity-purification mass spectrometry; AMPK, AMP-Activated Protein Kinase; C/EBPβ-LIP, CCAAT Enhancer Binding Protein Beta; CCR4-NOT, Carbon catabolite repression 4 (Ccr4)-negative on TATA-less (Not) Complex; CHOP, C/EBP-Homologous Protein 10; CUGBP1, CUG triplet repeat, RNA binding protein 1; DLK1/Pref1, Delta Like Non-Canonical Notch Ligand 1; DMIX1, Differentiation mix; DMEM, Dulbecco's modified Eagle's medium; FABF4, Fatty acid-binding protein 4; GSEA, Gene set enrichment analysis; HIF1A, Hypoxia inducible factor 1A; logCPM, Log2-counts per million; NFAT5, Nuclear factor of activated T-cells 5; ORO, Oil Red O; Plin1, Perilipin 1; PPARγ, Peroxisome proliferating-activated receptor gamma; TCEP, Tris (2-carboxyethyl) phosphine hydrochloride; TGFB1, Transforming growth factor beta; Sh, Short hairpin; SVF, Stromal vascular fraction; WAT, White adipose tissue.

* Corresponding author at: Department of Medical Biochemistry, Amsterdam University Medical Centers, Location AMC, Meibergdreef 15, 1105 AZ Amsterdam, the Netherlands.
E-mail address: c.j.devries@amsterdamumc.nl (C.J.M. de Vries).
[1] These authors have contributed equally to this work.
[2] Present address: Department of Anatomy and Stem Cells and Metabolism Research Program, Faculty of Medicine, University of Helsinki, Helsinki, Finland.
[3] These authors have contributed equally to this work.

https://doi.org/10.1016/j.cellsig.2023.110587
Received 31 October 2022; Received in revised form 25 December 2022; Accepted 3 January 2023
Available online 5 January 2023

1. Introduction

Mesenchymal stem cells can differentiate into distinct cell types such as adipocytes, myocytes, chondrocytes, and osteoblasts (1). The transition of precursor cells into cells with a mature cellular phenotype is orchestrated by the intricate expression pattern of cell-type-specific factors (2). Adipocyte differentiation occurs through two main phases: the commitment phase, when mesenchymal stem cells commit to the adipocyte lineage, and the terminal differentiation phase, which results in a unique adipocyte-specific gene expression profile and eventually the accumulation of lipid droplets in the cell (3). The adipocyte differentiation program involves a cascade of transcriptional events that regulate the expression of key proteins to establish the mature adipocyte phenotype. One of the key factors in adipocyte differentiation is the nuclear receptor peroxisome proliferating-activated receptor gamma (PPARγ) (4). Recently, it has been demonstrated that especially white adipose tissue (WAT) shows an extensive and relatively early differential gene expression pattern in aging mice (5). In addition, it has been proposed that peripheral fat loss with aging in humans involves defects in adipogenesis in the subcutaneous WAT depot (6). Overall, the differentiation capacity of pre-adipocytes gradually deteriorates with increasing age (7,8). The impaired pre-adipocyte differentiation has been linked to reduced levels of adipogenic factors such as C/EBP family members and PPARγ, but also to enhanced expression of for example AMP-Activated Protein Kinase (AMPK) and Delta Like Non-Canonical Notch Ligand 1 (DLK1/Pref1) (9,10). Given that pre-adipocyte (dys) function is a determinant of several human metabolic diseases (11), it is relevant that new factors and pathways that play a significant role in adipogenesis are still being discovered (12).

Four-and-a-Half LIM domains protein 2 (FHL2) is a member of the FHL subfamily of LIM-only proteins and is expressed in a wide variety of cells and tissues (13). FHL2 is a component of numerous signal transduction pathways acting through protein-protein interactions, thereby fine-tuning cellular processes (14). Recently, we demonstrated a novel function for FHL2 in energy metabolism, and more specifically in WAT (15). Using the mouse diet-induced obesity model, we observed that FHL2 deficiency in mice prevents weight gain, in part through enhanced browning of their WAT. FHL2 is also known to promote myoblast and osteoblast differentiation, through interaction with β-catenin and Wnt proteins, respectively (16–18). In the osteoblast study, it has been proposed that FHL2 deficiency may have an impact on adipocyte size, specifically in the bone marrow (16). However, a direct impact of FHL2 on adipogenesis has not been studied so far. Methylation of the human FHL2 gene is one of the strongest epigenetic DNA marks to identify the age of an individual, and FHL2 methylation is associated with an increased expression of this gene. Not only in blood but also in WAT, pancreatic β-cells, and skeletal muscle FHL2 methylation and expression is increased with aging (13). In the current study, we hypothesized that FHL2 plays a pivotal role in adipocyte differentiation. Therefore, the main aim of this study was to unveil a potential role for FHL2 in adipogenesis.

In two different models of adipogenesis *ex vivo* differentiated primary (pre)adipocytes and 3T3-L1 (pre)adipocyte cell line), we observed downregulation of FHL2 expression at the early stages of *in vitro* differentiation. Based on loss-of-function experiments (*ex vivo* differentiated FHL2−/− primary (pre)adipocytes) and overexpression experiments, we conclude that reducing FHL2 expression is essential for pre-adipocytes to undergo full differentiation into mature adipocytes. Considering that FHL2 exerts its biological functions through protein-protein interactions, we employed co-immunoprecipitation experiments followed by proteomics and identified the Nuclear factor of activated T-cells 5 (NFAT5) as a novel FHL2 interactor. NFAT5 has been reported to decrease adipocyte differentiation similarly to FHL2 (19,20), and we show that FHL2 requires NFAT5 to exert its function. In conclusion, we demonstrated a crucial role of FHL2 in adipogenesis and propose that FHL2 is a determinant factor in early adipogenesis and cell lineage commitment.

2. Materials and methods

2.1. Animals and Stromal Vascular Fraction (SVF) isolation

All animal experiments were approved by the ethics committee of the Amsterdam University Medical Center, The Netherlands, and were performed following European directive 2010/63/EU guidelines (permit number DBC287). FHL2-deficient mice (FHL2−/−) were generated by R. Bassel-Duby (University of Texas Southwestern Medical Center, Dallas, TX) and were bred onto a C57BL/6 background for >11 generations. Male littermates of 11-week-old were used, and *n* refers to the number of single animals. Littermates from wild-type and FHL2-deficient genotype were randomly separated in ventilated cages with free access to water and food. The suffering of animals was minimized as much as possible. The isolation of pre-adipocytes from the mouse SVF was performed as described previously (15). In short, excision of subcutaneous white adipose tissue depots was performed in WT and FHL2−/− mice, and the SVF was isolated to obtain pre-adipocytes for differentiation *in vitro*. The tissue was minced and digested in collagenase solution (1.5 mg/mL; Sigma-Aldrich; #C6885). After filtering and centrifuging, the pre-adipocytes were purified using a red blood cell lysis buffer (Roche; # 11814389001) and neutralized with Dulbecco's modified Eagle's medium (DMEM) (Gibco, Thermo Fisher; #41965062) supplemented with 10% FBS and 1% penicillin-streptomycin. Finally, cells were centrifuged again and seeded in cell culture plates for differentiation.

2.2. 3T3-L1 cell culture and pre-adipocyte differentiation

The 3T3-L1 cell line (ATCC: CL-173) was cultured in DMEM supplemented with 10% FBS and 1% penicillin-streptomycin at 37 °C and 5% CO_2. The protocol for pre-adipocyte differentiation was performed as described elsewhere (21), and it was used for both 3T3-L1 and SVF pre-adipocyte differentiation. Cells were grown to confluency and after 2 days culture medium supplemented with differentiation mix 1 (DMIX1) was added to the cells for 2 days (DMIX1 contains: 500 μM of isobutyl-1-methylxanthine (IBMX), 1 μM of dexamethasone, and 170 nM of insulin). On day 4, DMIX1 was replaced by differentiation mix 2 (DMIX2; culture medium containing 170 nM of insulin) and this was replaced regularly until day 8 of differentiation.

2.3. Lentiviral transduction

Recombinant lentiviral particles encoding FHL2 with GFP tag (FHL2-GFP), only the GFP tag as control (CTRL-GFP), and two different constructs of shRNA targeting mouse NFAT5 (shNFAT5–1 target sequence is 5′- GCAGAACAACATCCCTGGAAT-3′ and, shNFAT5–2 target sequence is 5′- CCACCATGTTTCAGACACCAA-3′), as well as one without NFAT5 as control (shCTRL), were produced, concentrated, and titrated as described previously (22). Cells were seeded at 70–80% confluency and incubated with recombinant lentivirus for 24 h. After 24 h, the medium was refreshed, and cells were cultured using medium containing 1 μg/mL of the selection marker puromycin (for the GFP constructs) or 500 μg/mL of neomycin (for the shNFAT5 constructs). After 3–10 days resistant cells were further expanded for experiments.

2.4. RNA isolation and reverse transcription (RT)-qPCR

Total RNA isolation from cultured cells was performed using TRI Reagent® (Sigma Aldrich; #T9424). Then, cDNA was synthesized using iScript™ cDNA Synthesis Kit (BioRad; #1708890). Quantitative PCR was carried out using a LightCycler 480 II PCR platform (Roche) with the correspondent pair of primers (sequences listed in Table S1) and SensiFAST SYBR No-ROX Kit (Bioline; #BIO-98050). Cycle

quantification and amplification efficiency were calculated using the LinReg PCR software package (23) and Rplp0 and β-actin were used as housekeeping genes to normalize target gene expression.

2.5. RNA sequencing

Cells transduced with lentiviral particles and stably expressing CTRL-GFP or FHL2-GFP were differentiated for 2 days as described before. RNA isolation from these cultured cells was performed using TRI Reagent® according to the manufacturer's protocol. Libraries were prepared using Truseq RNA stranded polyA (Illumina) and sequenced on an Illumina nextseq2000 in paired-end 50 bp reads. Reads were subjected to quality control (FastQC, dupRadar), trimmed using Trimmomatic v0.39, and aligned to the genome using HISAT2 (v2.2.1) (24–26). Counts were obtained using HTSEq. (v0.11.0) using the corresponding GTF. Statistical analyses were performed using the edgeR and limma/voom R packages. Count data were transformed to log2-counts per million (logCPM), normalized by applying the trimmed mean of M-values method and precision weighted using voom. Differential expression was assessed using an empirical Bayes moderated *t*-test within limma's linear model framework including the precision weights estimated by voom. The resulting *p* values were corrected for multiple testing using the Benjamini-Hochberg false discovery rate. Genes were re-annotated using biomaRt using the Ensembl genome databases. Geneset enrichment is performed with MSigDB genesets using CAMERA approach as implemented in limma (27), and applying the Geneset Enrichment Analysis (GSEA) tool. The resulting DEGs, expression plots, and geneset enrichment results are shown in an in-house made Shiny-app. The raw and processed RNA-seq data have been deposited in the Gene Expression Omnibus (GEO) database under accession number GSE200920.

2.6. Western blotting

Proteins from cultured cells were obtained using RIPA lysis buffer (150 mM NaCl, 50 mM Tris pH 7.4, 1% IGEPAL-CA630, 0.5% sodium deoxycholate, 0.1% SDS and Roche cOmplete™ protease inhibitor cocktail). Concentration was calculated using the DC protein assay (BioRad; #5000111) to load equal amounts of sample into SDS-PAGE gels. After transferring to nitrocellulose membranes, these were blocked with 2% non-fat milk for 1 h and incubated overnight at 4 °C with the corresponding primary antibody (Mouse anti-FHL2 - #MA1–40200 from ThermoFisher, Rabbit anti-NFAT5 - #ab3446 from Abcam, Rabbit anti-HA tag - #3724S from Cell Signaling, Mouse anti-c-Myc tag - #sc-40 from Santa Cruz and Mouse anti-alpha-tubulin - #CLT9002 from Cedarlane as loading control). After washing the membranes, they were incubated with the appropriate HRP-conjugated secondary antibody at room temperature for 1 h. Visualization of protein bands was done in ImageQuant 800 imager using SuperSignal West Pico PLUS Chemiluminescent Substrate (ThermoScientific #34579), and quantification of band intensity was possible using the ImageJ Gel Analysis software.

2.7. Intracellular lipid staining and immunofluorescence staining

To stain lipid accumulation in 3T3-L1 cells, we used two different methods: Oil Red O (ORO) staining and HCS LipidTOX Deep Red Neutral Lipid Stain (Invitrogen; #H34477), both methods stain neutral lipids in cultured cells. For the ORO staining, cells were fixed for 20 min at room temperature using 4% formalin. Fixative was removed and after washing again with PBS, the 0.2% ORO solution was added to the wells and incubated for 30 min at room temperature. After this, cells were washed several times with distilled water. For quantification, the dye was eluted using 100% 2-propanol, and absorbance was measured at 510 nm in triplicate. For LipidTOX staining, cells were grown on gelatin-coated glass coverslips and fixated as described before. Then, coverslips were incubated with LipidTOX (1:150 dilution) and DAPI nuclear staining (1:1000) for 30 min at room temperature. After washing, coverslips were mounted on slides and imaged. For immunofluorescence, cells were cultured on gelatin-coated glass coverslips for differentiation. On different days of differentiation, cells were fixed in 4% paraformaldehyde (Roth) for 20 min at room temperature. After the addition of 0.5% Triton X-100 for 5 min to permeabilize the nuclei, samples were blocked with 2% BSA and incubated with primary antibody (Rabbit anti-NFAT5 - #ab3446 from Abcam) and DAPI nuclear staining. Then, following washing and incubation with secondary (Alexa-488 goat anti-Rabbit) the samples were mounted in slides for imaging using a Nikon ECLIPSE Ti microscope with standard DAPI, GFP, and mCherry filter cubes. Images were processed using ImageJ Gel Analysis software.

2.8. Co-immunoprecipitation

HEK-293 T cells were co-transfected with HA-tagged FHL2 and myc-tagged NFAT5 plasmids using the CalPhos Mammalian Transfection Kit (Takara; #631312) and incubated for 48 h. For the LIM mutants, plasmids encoding different numbers of FHL2 LIM-domains (HA-tagged LIM0–1, LIM0–2, and LIM0–3) (28) were co-transfected together with myc-tagged NFAT5. Then, protein lysates were obtained using NP-40 lysis buffer (1% (*v*/v) Nonidet P-40, 50 mM Tris-HCl, 100 mM NaCl, 10% (v/v) glycerol) supplemented with protease and phosphatase inhibitors. After calculating protein concentration, lysates were incubated with pull-down antibody (Rabbit anti-HA tag - #3724S from Cell Signaling) overnight at 4 °C. The next day, the complex was incubated for 2 h with magnetic Dynabeads® Protein G (ThermoFisher; #10003D). Immunoprecipitates were then washed and eluted from the beads and analyzed by western blotting.

2.9. Mass spectrometry

Precipitated proteins were denatured and alkylated in 50 μl 8 M Urea, 1 M ammonium bicarbonate (ABC) containing 10 mM TCEP (tris (2-carboxyethyl) phosphine hydrochloride) and 40 mM 2-chloro-acetamide. After 4-fold dilution with 1 M ABC and digestion with trypsin (250 ng/200 μl), peptides were separated from the beads and desalted with homemade C-18 stage tips (3 M, St Paul, MN), eluted with 80% Acetonitrile (ACN) and, after evaporation of the solvent in the speedvac, redissolved in buffer A (0,1% formic acid). After separation on a 30 cm pico-tip column (75 μm ID, New Objective) in-house packed with C-18 material (1.9 μm aquapur gold, dr. Maisch) using a 140 min gradient (7% to 80% ACN, 0.1% FA), delivered by an easy-nLC 1200 (Thermo), peptides were electro-sprayed directly into a Orbitrap Eclipse Tribrid Mass Spectrometer (Thermo Scientific), that was run in DDA mode with a cycle time of 1 s, with the FAIMS compensation voltage (CV) switching between -45 V and -65 V. The full scan (400–1400 mass range) was performed at a resolution of 240,000. Ions reaching an intensity threshold of 10E4, were isolated by the quadrupole with na 0.8 Da window, fragmented with a HCD collision energy of 30% and measured in de Iontrap on rapid mode.

After splitting of the raw files into the two CV channels with Freestyle Software (Thermo), analysis of the raw data was performed with MaxQuant (1.6.3.4), using the Uniprot fasta file (UP000000589) of *Mus musculus* (taxonomy ID: 10090) (2020 Jan 21). To determine proteins of interest, we performed a differential enrichment analysis. We filtered for proteins that were identified in at least two out of three of the replicates of one condition and background corrected and normalized the data by variance stabilizing transformation. We used a left-shifted Gaussian distribution to impute for missingness since our data presented a pattern of missingness not at random (MNAR). Finally, we performed a *t*-test with multiple testing correction using a Benjamini-Hochberg FDR approach set to 0.5%. The program used for the analyses was R [version 4.0.4] through R-Studio [version 1.5.64]. The mass spectrometry proteomics data have been deposited to the ProteomeXchange Consortium

via the PRIDE partner repository with the dataset identifier PXD033974 (http://www.ebi.ac.uk/pride). Then, differential enrichment analysis was created to identify those proteins that were over-enriched and selected those with at least a 2.5-fold change and adjusted *p*-value ≤0.05.

2.10. Reporter assays

Transient transfection of HEK-293 T cells with pcDNA3.1-Gal4DBD-NFAT5, pCMV-HA-FHL2, and pCMV-HA-LIM0–2 (28), pGL3 reporter, and TK-Renilla luciferase was performed using Xtreme gene 9 DNA transfection reagent (Roche; #XTG9-RO). Following incubation for 48 h, cells were lysed and the Dual-Luciferase Reporter Assay System (Promega) was used to measure luciferase in a TriStar2 LB942 Multimode Reader. Independent experiments were performed three times.

2.11. BrdU proliferation assay

The proliferation of 3T3-L1 cells was determined using the BrdU cell proliferation ELISA (Roche; #11647229001) according to the manufacturer's protocol. An equal number of cells stably overexpressing CTRL-GFP or FHL2-GFP were labeled with BrdU for 2 h. After fixation, samples were incubated with a peroxidase-conjugated anti-BrdU antibody. Next, samples were washed and incubated with the substrate solution for colour development. The reaction was stopped after 10–20 min, and absorbance was measured at 450 nm.

2.12. Statistical analysis

Statistical analyses were performed using GraphPad Prism software. Data are presented as mean ± SEM. *P*-values were calculated using Student's *t*-test, or two-way ANOVA with Tukey's posthoc correction if data were normally distributed. A *p*-value <0.05 was considered statistically significant.

3. Results

3.1. FHL2 is expressed in WAT and expression is regulated during early differentiation of 3T3-L1 cells

To examine the expression of FHL2 in the different cell types in adipose tissue, subcutaneous WAT from wild-type C57BL/6 mice was separated into mature adipocytes and the stromal vascular fraction (SVF); the latter fraction contains immune cells, endothelial cells, and pre-adipocytes. FHL2 mRNA is expressed in both SVF (containing pre-adipocytes) and in the mature adipocyte fraction, with the highest expression in SVF (Fig. 1A). Therefore, we hypothesized that FHL2 expression might be regulated during adipocyte differentiation. To address this in an independent experimental model, we applied the 3T3-L1 cell line, a standard model to study adipogenesis (29,30). Cells were differentiated for 8 days using standard hormonal cocktails and we confirmed a successful differentiation based on the expression of key adipogenic markers such as PPARγ and its target genes adiponectin (ADIPOQ) and fatty acid-binding protein 4 (FABP4) (Fig. 1B). During differentiation, FHL2 is transiently downregulated at day 2 of differentiation both at the mRNA and protein level (Fig. 1C-D), this being the moment that the adipogenic cocktail (here named differentiation mix or DMIX1) is added to trigger the initiation of adipocyte differentiation. Based on this observation, we decided to dissect which specific component of the DMIX1 causes this regulation of FHL2 expression. 3T3-L1 cells were incubated with separate components of the mix and we demonstrated that IBMX, which enhances intracellular cAMP levels, causes the decrease in FHL2 expression, whereas dexamethasone and insulin do not affect FHL2 expression (Fig. 1E). In conclusion, FHL2 is expressed in pre-adipocytes and is downregulated in the early stages of *in vitro* pre-adipocyte differentiation.

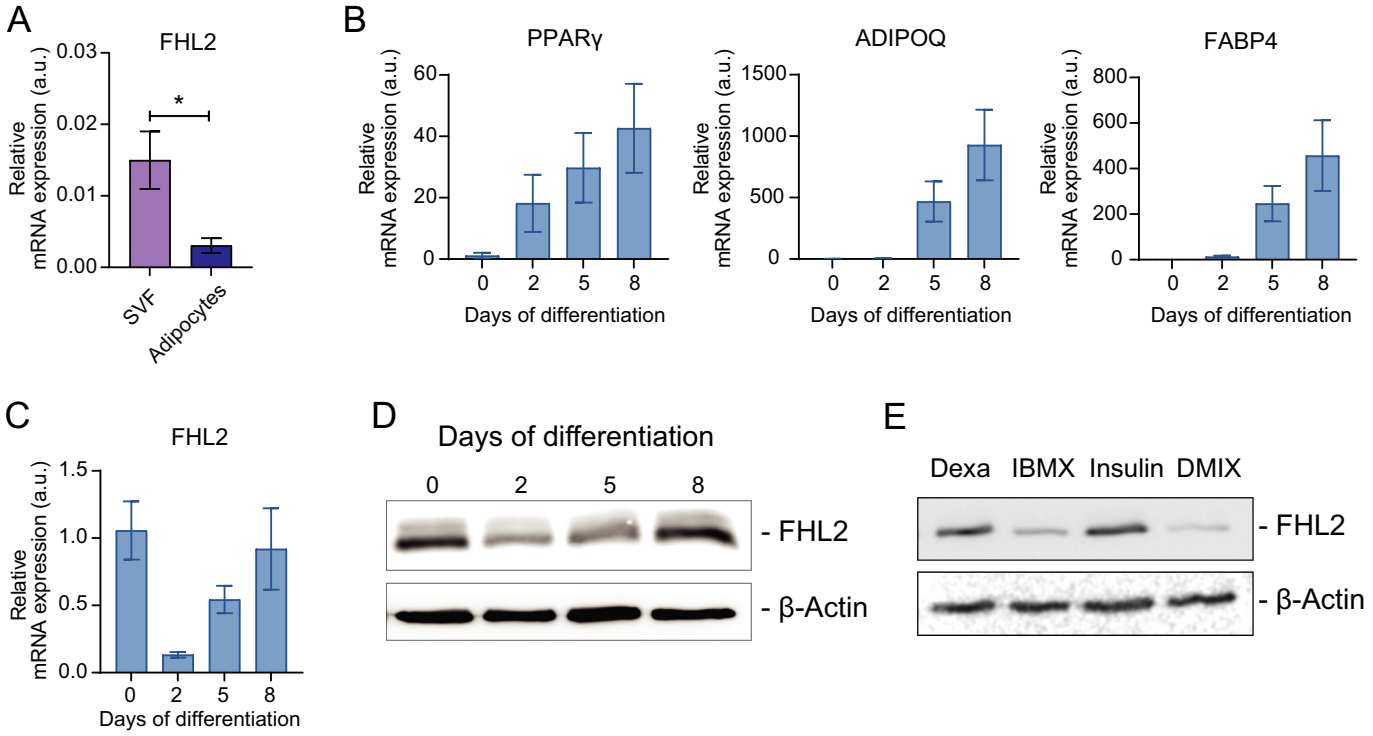

Fig. 1. FHL2 expression in mouse adipose tissue fractions and 3T3-L1 adipocyte differentiation. **A)** Relative mRNA expression of FHL2 in pre-adipocytes from the SVF and in mature adipocytes. **B and C)** Relative mRNA expression of PPARγ, ADIPOQ, FABP4, and FHL2 during 8 days of differentiation of 3T3-L1 cells, where cells were cultured to confluency before receiving 2 days of treatment with DMIX1 and later maintained with DMIX2 until day 8 (section 2.2). **D)** Western blot to reveal FHL2 protein expression during 3T3-L1 differentiation (β-actin used as loading control). **E)** FHL2 protein expression in cells treated with Dexamethasone (1 μM), IBMX (500 μM), Insulin (170 nM), or full differentiation mix (DMIX1) for 2 days before protein harvest. Data are indicated as mean ± SEM (*$p < 0,05$).

3.2. FHL2 overexpression inhibits adipocyte differentiation

To study the role of FHL2 in adipocyte differentiation in more detail, we used full-body FHL2-deficient mice and their wild-type littermates as control, FHL2−/− and WT mice; to isolate the pre-adipocytes from WAT and induce differentiation towards mature adipocytes. Similar to 3T3-L1 cells (Fig. 1 C and D), FHL2 expression is downregulated at day 2 in WT pre-adipocytes during differentiation (Fig. 2A), but we did not find any difference in adipocyte differentiation between WT and FHL2−/− pre-adipocytes based on the expression of the aforementioned adipocyte markers PPARγ, ADIPOQ, and FABP4 (Fig. 2B) nor lipid accumulation (data not shown). Therefore, we conclude that FHL2 deficiency does not alter the overall adipogenic capacity of mouse pre-adipocytes. However, given the transient and dramatic decline in FHL2 expression during early differentiation, we hypothesized that this reduction of FHL2 levels may present an essential step in adipogenesis. To investigate this, we constitutively overexpressed GFP-tagged FHL2 or GFP through stable lentiviral transduction in 3T3-L1 cells (Fig. 2C, Fig. S1A). Next, these cell lines were subjected to the differentiation protocol and we observed that cells constitutively expressing FHL2-GFP did not differentiate properly, based on reduced intracellular lipid accumulation using LipidTOX staining after 5 days (Fig. 2D) and by Oil Red O lipid staining followed by quantification (Fig. S1B). Moreover, mRNA analyses showed that even though the early adipogenic marker CEBPβ is not different between groups, the expression of the late adipogenic markers PPARγ, ADIPOQ, and FABP4 is drastically inhibited in FHL2-GFP cells (Fig. 2E). Since cell differentiation often antagonizes cell proliferation (31), we evaluated whether FHL2 overexpression affects cell proliferation in these cells, but we did not observe any difference between GFP and FHL2-GFP cells (Fig. S1C). These experiments established that whereas lack of FHL2 has no apparent effect on adipocyte differentiation, constitutive expression of FHL2 prevents differentiation of pre-adipocytes into mature adipocytes, keeping them in an immature state.

3.3. FHL2 overexpression alters gene transcription in early differentiation

Given that FHL2 overexpression effectively represses differentiation, we next aimed to assess the effect of elevated FHL2 levels on the

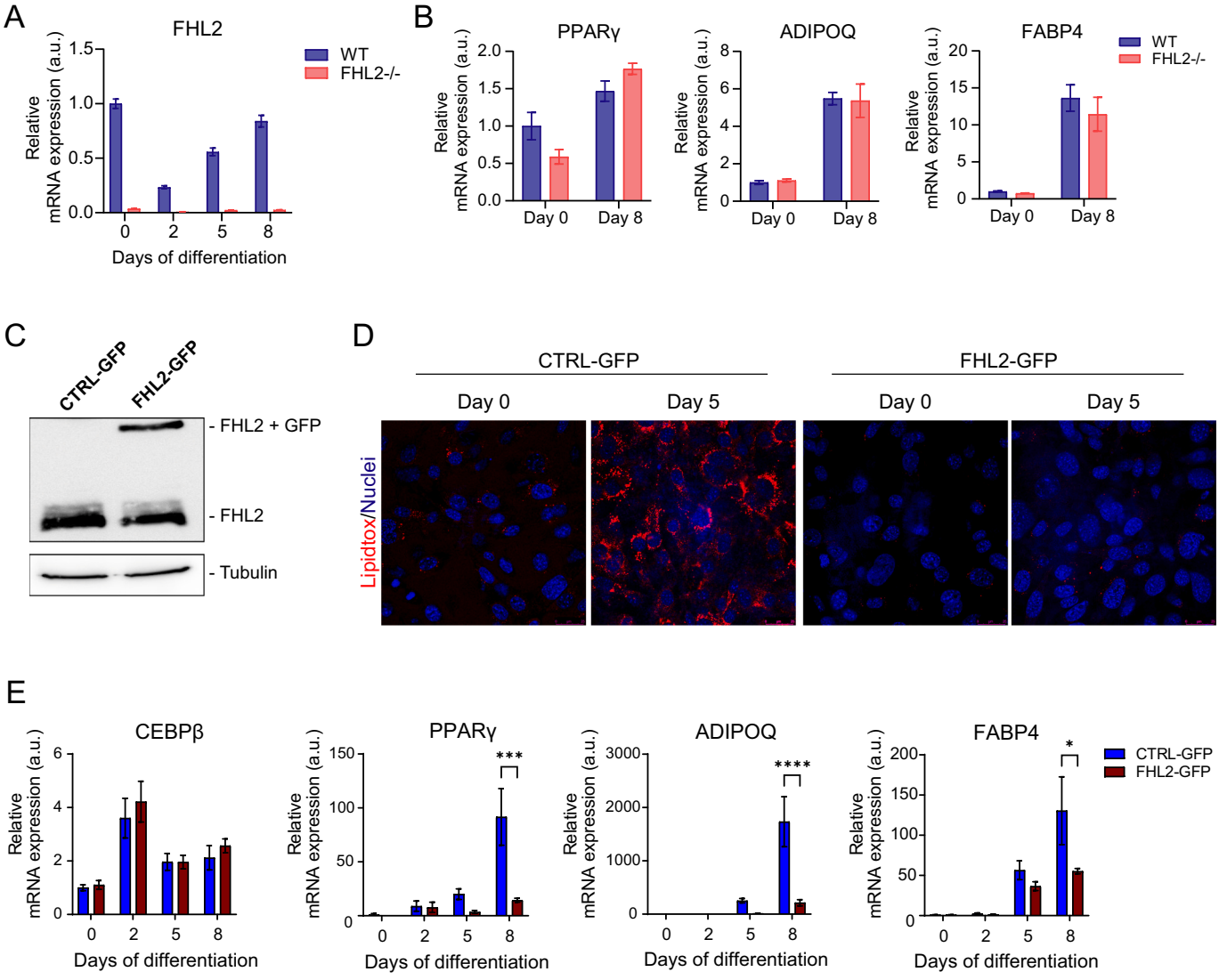

Fig. 2. FHL2 overexpression inhibits the differentiation of pre-adipocytes. **A)** Relative mRNA expression of FHL2 during differentiation of pre-adipocytes derived from WT ($n = 3$) and FHL2−/− (n = 3) mice. **B)** Relative mRNA expression of PPARγ, ADIPOQ, and FABP4 at days 0 and 8 of differentiation of WT and FHL2−/− pre-adipocytes. **C)** Western blot to visualize protein expression of endogenous FHL2 and overexpressed FHL2-GFP in 3T3-L1 cells (tubulin used as loading control). **D)** Intracellular lipids (red) and nuclear DAPI (blue) staining of CTRL-GFP and FHL2-GFP 3T3-L1 cells at days 0 and 5 of differentiation. **E)** Relative mRNA expression of CEBPβ, PPARγ, ADIPOQ, and FABP4 during 8 days of differentiation of CTRL-GFP and FHL2-GFP cells. Data are indicated as mean ± SEM (*p < 0,05). (For interpretation of the references to colour in this figure legend, the reader is referred to the web version of this article.)

transcriptome of 3T3-L1 cells during the early stages of differentiation. We performed RNAseq transcriptomic analysis of confluent cell cultures before (day 0) and two days after the addition of the adipocyte differentiation cocktail necessary to start differentiation (DMIX1; Fig. 3A). The largest difference in terms of the number of differentially expressed genes between cells expressing FHL2-GFP and control cells (CTRL-GFP) was found on day 2 when 473 genes are significantly upregulated and 651 genes are downregulated. In contrast, 141 and 274 genes were found to be significantly up- and down-regulated at day 0, respectively (Fig. 3B), indicating that the main effect of FHL2 at the transcriptional level occurred after 2 days of differentiation. In Fig. 3C-D, volcano plots with several genes are indicated as the top differentially expressed genes in FHL2-GFP cells. At day 2, the top downregulated genes include well-established adipogenesis marker genes including the Pparγ target genes Adipoq, Perilipin 1 (Plin1), and Adipsin (Cfd), confirming the inhibition of adipogenesis upon FHL2 overexpression (Fig. 2). Extensive pathway analyses (Fig. 3E, Fig. S2A—B) revealed that adipogenic pathways, as well as other pathways that have been described to participate in adipocyte differentiation or lineage commitment, such as HIF1A targets and Response to TGFB1 (32,33), are downregulated upon constitutive FHL2 expression during differentiation. A heatmap of genes involved in adipogenesis illustrates the repressive effect of FHL2 on the expression of these genes (Fig. 3F). Detailed gene set enrichment analysis (GSEA) of these data further illustrate these findings (Fig. 3G). These transcriptomic data strongly support our finding that constitutive FHL2 expression results in inhibition of early adipocyte differentiation.

3.4. FHL2 interacts with the nuclear factor of activated T-cells 5 (NFAT5) in 3T3-L1 cells

As FHL2 does not bind DNA by itself but modulates gene transcription through interaction with transcription factors (34), we wished to identify with which proteins FHL2 interacts to inhibit adipogenesis. We applied GFP-mediated affinity-purification mass spectrometry (AP-MS) to identify FHL2 interactors in 3T3-L1 cells, using an optimized technique (35), with GFP overexpressing cells as a control. Using this approach, we identified 51 significant interactors, some of which are shown in Table S2, for FHL2 in 3T3-L1 cells. In Fig. 4A the results are presented in a volcano plot with the most significant interactors indicated. The presence of FHL2 among this set of proteins confirms the specificity of this approach. Among the most significant interacting protein, we detected the nuclear factor of activated T-cells 5 (NFAT5), a transcription factor previously implicated in adipogenesis (19,20,36), and eight members of the carbon catabolite repression 4 (Ccr4)-negative on TATA-less (Not) complex, referred to as the CCR4-NOT or CNOT complex, a large, highly conserved, multifunctional assembly of proteins that is predominantly involved in the regulation of mRNA stability (37,38). As NFAT5 has been shown to inhibit adipocyte differentiation and WAT browning (19,20,36), reminiscent of the function of FHL2 in adipocytes as presented in the current study and our previous study (15), we decided to focus on the interaction between FHL2 and NFAT5. First, we assessed the expression pattern of NFAT5 during adipocyte differentiation in more detail and examined whether its expression was altered upon overexpression of FHL2. NFAT5 shows a similar downregulation of expression at day 2 as FHL2, and overexpression of FHL2-GFP does not alter NFAT5 expression (Fig. 4B). To confirm the interaction observed in the AP-MS experiments between FHL2 and NFAT5, co-immunoprecipitation was performed for HA-tagged FHL2 and Myc-tagged NFAT5 (Fig. 4C). It is worth to mention that for this experiment same amount of DNA and cells was used across the different conditions, but the result shows enhanced expression levels of FHL2-HA and NFAT5-Myc when co-expressed, which suggests some degree of protein stabilization. Moreover, in this experiment three different mutants of FHL2 were included in which one or more LIM domains are missing; LIM0–1, LIM0–2, and LIM0–3. We observed that the LIM mutant lacking the last LIM domain (LIM0–3) was the only mutant, in addition to full-length FHL2, interacting with NFAT5 albeit to a lesser extent (Fig. 4D).

Given that NFAT5 is a transcription factor, we assessed whether the interaction between FHL2 and NFAT5 affects the transcriptional activity of NFAT5. First, we performed immunofluorescence staining for FHL2 and NFAT5 in 3T3-L1 cells and demonstrated that FHL2 is localized throughout the cell and that both proteins co-localize in the nucleus (Fig. 4E). As NFAT proteins are widely expressed (39), we next employed a Gal4-reporter assay to perform transcriptional activity assays, to avoid interference of endogenous NFAT proteins. Fusion of the Gal4 DNA-binding domain to NFAT5 resulted in a protein that activates a Gal4-luciferase reporter. The activity of Gal4-NFAT5 is reduced upon overexpression of FHL2, but not when the LIM0–2 variant of FHL2, which fails to interact with NFAT5 (Fig. 4D), was used (Fig. 4F). These data confirm that the interaction between NFAT5 and full-length FHL2 is functional.

3.5. FHL2 inhibition of adipocyte differentiation involves cooperation with NFAT5

Lee et al. (20) demonstrated that NFAT5 inhibits adipogenesis by blocking the expression of the PPARγ gene, similar to what FHL2 does after overexpression during differentiation. As both FHL2 (Fig. 2) and NFAT5 (19,20) inhibit adipogenesis, and because these proteins functionally interact (Fig. 4), we considered that FHL2 and NFAT5 operate through a common cellular pathway. To examine this, we knocked down NFAT5 expression in CTRL-GFP and FHL2-GFP overexpressing cells using two different short-hairpin constructs (shNFAT5–1 and shNFAT5–2), resulting in approximately 40% knockdown of NFAT5 compared to the corresponding control (shCTRL) (Fig. 5A). We first confirmed that this level of inhibition of NFAT5 expression in 3T3-L1 cells leads to enhanced adipogenesis, as illustrated by the strong upregulation of FABP4 expression (Fig. 5B) (20). While FABP4 expression is inhibited in FHL2 overexpressing cells (Fig. 2E), simultaneous knockdown of NFAT5 resulted in a rescue of FABP4 expression for both short hairpins on both the mRNA and protein level (Fig. 5B-C and Fig. S4). Other differentiation markers (ADIPOQ and PPARγ) gave comparable results, with some variation between the two short hairpins used (Fig. S3A—B, Fig.S4 and Fig. 5C). To underscore the recovery of the FHL2-mediated inhibition of adipogenesis by reducing NFAT5 expression, we performed an intracellular lipid staining showing that FHL2 overexpression inhibits lipid loading of the cells unless NFAT5 expression is knocked down (Fig. 5D). Overall, these experiments support the conclusion that inhibition of adipogenesis in FHL2 overexpressing cells involves its interaction with NFAT5. In the absence of NFAT5, FHL2 can no longer inhibit PPARγ expression, and thus no longer affect the differentiation of 3T3-L1 cells. In conclusion, our data support a model where downregulation of the FHL2-NFAT5 pathway presents an essential step in early adipogenesis (Fig. 6).

4. Discussion

Pre-adipocyte differentiation is a highly-regulated and complex process requiring the sequential expression of a considerable number of proteins, ultimately resulting in the generation of mature adipocytes. The expression of crucial proteins occurs in a specific chronological order during the distinct stages of adipogenesis with for example the transcription factor CEBPβ playing a crucial role during the early stages, while PPARγ is a key player at later stages (40). Furthermore, multiple proteins have been identified to inhibit adipogenesis, like AMPK, C/EBPβ-LIP, CHOP, and CUGBP1 (6,9,10). Any alteration in this intricately regulated gene expression profile affects the formation of mature adipocytes, either promoting or inhibiting appropriate differentiation (9,10,41,42). In the current study, we discovered that the multifaceted protein FHL2 is transiently downregulated during the early stages of adipocyte differentiation, which is essential to achieving full

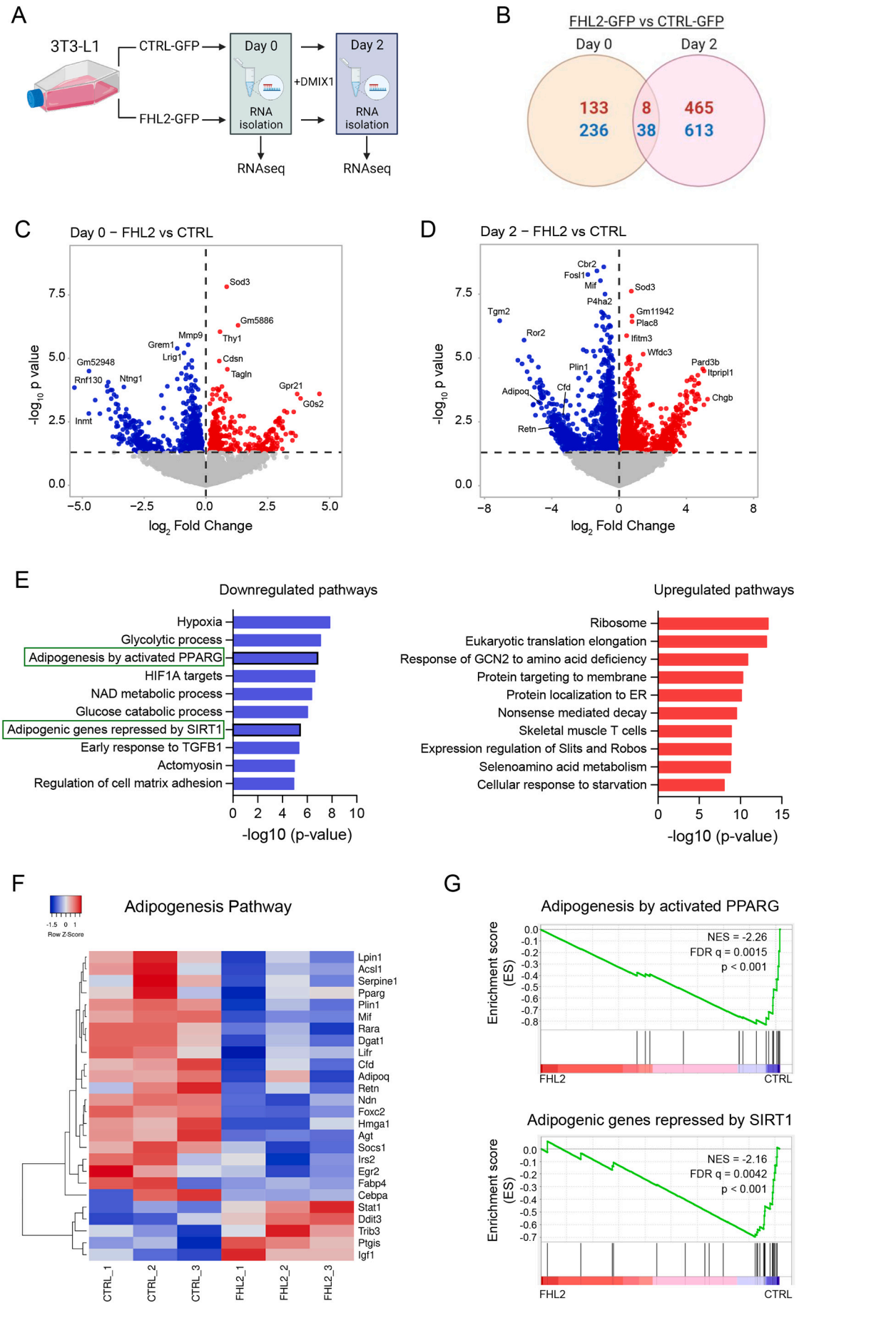

(caption on next page)

Fig. 3. Transcriptional changes in FHL2-GFP and control 3T3-L1 cells. **A)** Experimental setup scheme. **B)** Venn diagram of differentially expressed genes of FHL2-GFP *vs* CTRL-GFP comparison at days 0 and 2 of differentiation (*p*-value <0.05). Upregulated genes in red and downregulated genes in blue. **C)** Volcano plot of RNAseq at day 0 and **D)** day 2 of differentiation (FHL2-GFP *vs* CTRL-GFP). **E)** Top up- and down-regulated pathways in FHL2-GFP cells at day 2 of differentiation. **F)** Heatmap depicting the gene expression pattern of the Adipogenesis pathway at day 2 in CTRL-GFP and FHL2-GFP cells. **G)** Significant GSEA Enrichment Score curves (in green) from two adipogenic pathways: Adipogenesis activated by PPARG (GSEA: C2_M1645) and Adipogenic genes repressed by SIRT1 (GSEA: C2_M2183). Genes on the far left (red) correlated with FHL2-GFP cells, and genes on the far right (blue) correlated with CTRL-GFP cells. The vertical black lines indicate the position of each gene in the studied gene set. The normalized enrichment score (NES), false discover rate (FDR), and nominal p-value are shown for each pathway. (For interpretation of the references to colour in this figure legend, the reader is referred to the web version of this article.)

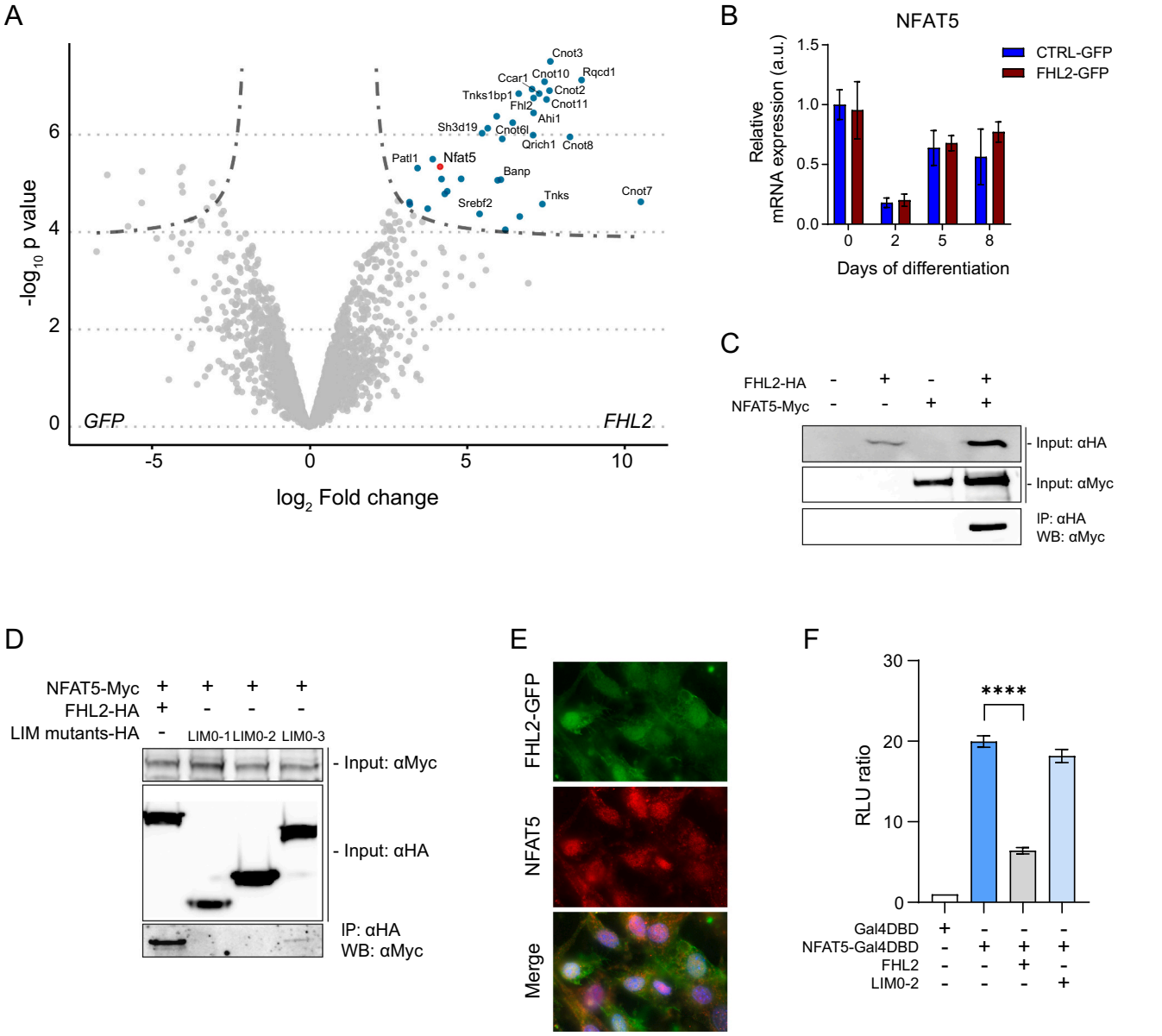

Fig. 4. NFAT5 and FHL2 interact in 3T3-L1 cells. **A)** Volcano plot showing FHL2-GFP interacting proteins detected in the AP-MS experiment, compared to the GFP control results in 3T3-L1 cells. **B)** Relative mRNA expression of NFAT5 during 8 days of differentiation in CTRL-GFP and FHL2-GFP 3T3-L1 cells. **C)** Co-immunoprecipitation assay of FHL2-HA and NFAT5-myc in HEK-293T cells. Equal number of cells were transfected using the same amount of DNA through all conditions. **D)** Co-immunoprecipitation assay of LIM mutants (LIM0–1, LIM0–2, and LIM0–3) and NFAT5-Myc in HEK-293 T cells. **E)** Fluorescence of FHL2-GFP (green), and immunofluorescence of NFAT5 (red), merged with nuclear DAPI (blue) in confluent 3T3-L1 cells. **F)** Gal4-reporter assay of NFAT5-Gal4DBD, FHL2, and LIM mutants LIM0–2. Data normalized using Renilla luciferase. Data are indicated as mean ± SEM (*p < 0,05). (For interpretation of the references to colour in this figure legend, the reader is referred to the web version of this article.)

differentiation. More specifically, we demonstrated that FHL2 expression is downregulated in two distinct adipocyte differentiation systems; in pre-adipocytes isolated from the SVF of mouse WAT, as well as in the 3T3-L1 cell line. The latter cell line is an extensively used model to study adipogenesis where cells are already committed to some extent to the adipocyte lineage (3).

We found that one of the components of the differentiation cocktail, IBMX, is sufficient to incite downregulation of FHL2 expression, indicating that increased intracellular cAMP inhibits the expression of FHL2 in pre-adipocytes. Further studies are required to identify the

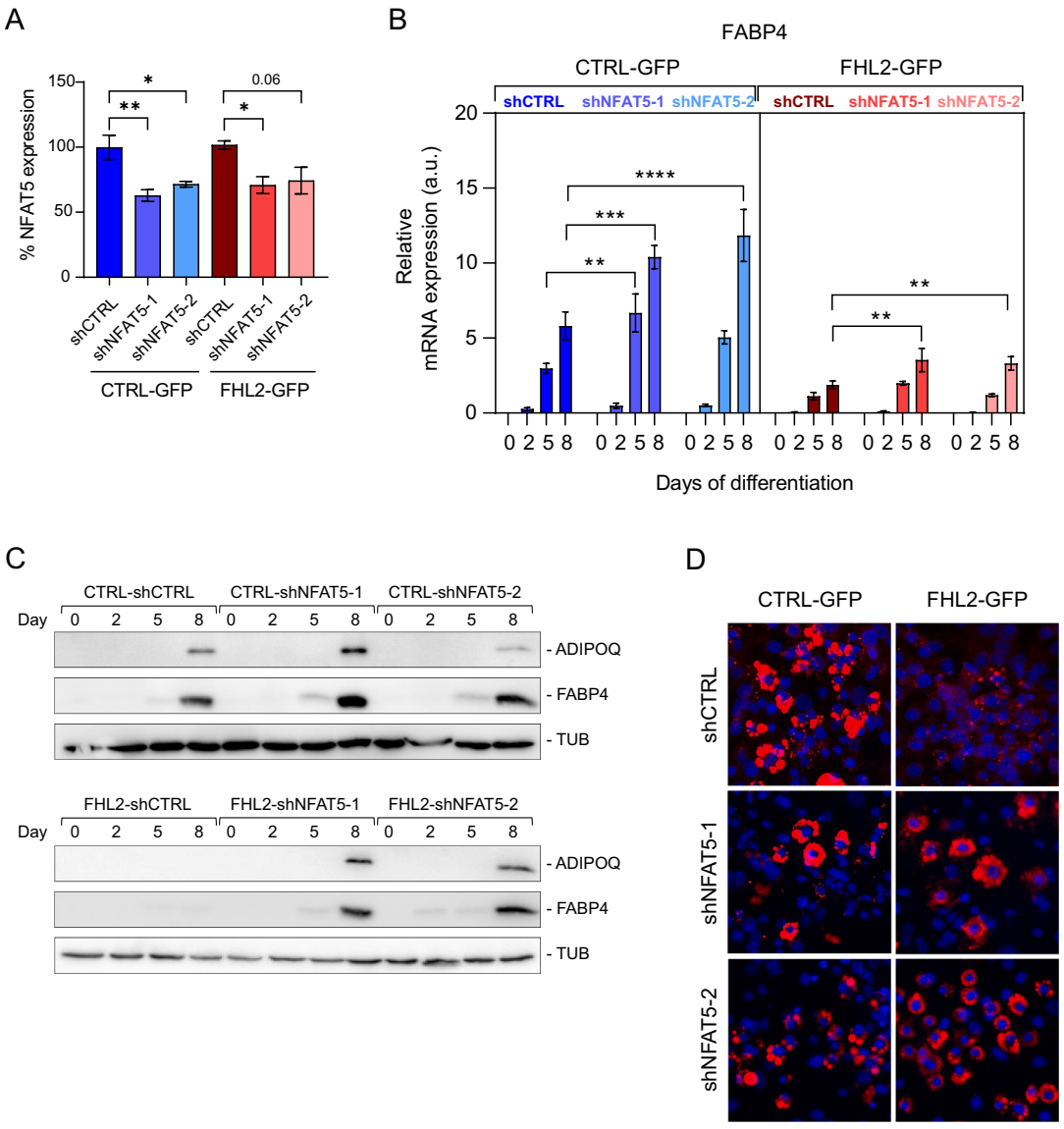

Fig. 5. FHL2 overexpression inhibits adipogenesis through interaction with NFAT5. **A)** Relative mRNA expression of NFAT5 in CTRL-GFP and FHL2-GFP cells that were transduced with shCTRL or two different short hairpins for NFAT5 (shNFAT5–1 and shNFAT5–2). **B)** Relative mRNA expression of FABP4 in CTRL-GFP and FHL2-GFP transduced with shCTRL, shNFAT5–1, or shNFAT5–2. **C)** Western blot of FABP4, Adiponectin, and Tubulin in FHL2-GFP transduced with shCTRL, shNFAT5–1, or shNFAT5–2 cells during 8 days of differentiation. **D)** Immunofluorescence staining of intracellular lipids (red) and nuclear DAPI (blue) in differentiated cells. Data are indicated as mean ± SEM (*p < 0,05). (For interpretation of the references to colour in this figure legend, the reader is referred to the web version of this article.)

physiological stimulus triggering an intracellular cAMP increase in pre-adipocytes and to clarify which specific cAMP-dependent factor(s) or pathways trigger downregulation of FHL2 expression, both in cellular differentiation assays and *in vivo*. To substantiate that the decrease in FHL2 expression is essential for adipogenesis, we constitutively overexpressed FHL2, resulting in a complete block of the differentiation process. In line with the crucial downregulation of FHL2 expression to allow adipocyte differentiation, we demonstrated that the differentiation of pre-adipocytes derived from FHL2-deficient mice occurs normally. It is important to mention that FHL2 has a function in mature WAT, as we demonstrated recently (15). More specifically, in mice FHL2 regulates the 'browning' of WAT, thereby affecting the energy expenditure of this tissue, which may contribute to the extent of weight gain of the mice when exposed to a high-fat diet (15). Furthermore, also in humans, the expression level of FHL2 in WAT is associated with 'browning' genes.

Upon constitutive expression of FHL2, the adipogenic program involving the expression of PPARγ and its target genes ADIPOQ and FABP4 is blunted, as well as the final lipid loading of the cells. Taking into account that FHL2 acts through protein-protein interactions, we investigated the interactome of FHL2 in 3T3-L1 cells using a mass spectrometry method and identified NFAT5. This protein is part of the Rel family of transcription factors and is also known as a 'tonicity-responsive enhancer-binding protein' because it is involved in the cellular response to hypertonic stress (43). NFAT5 also has a function in the immune response, especially in T cells and macrophages (44). However, what made us particularly interested in this interaction partner, is its role in adipogenesis and adipose tissue (19,20,36). In 3T3-L1 cells, NFAT5 has been reported to bind to the PPARγ promoter and block PPARγ expression (20). In addition, the reduction of NFAT5 expression promotes a faster activation of the adipogenic program, whereas its overexpression inhibits adipogenesis (19,20). This analogous behavior of NFAT5-overexpressing cells and FHL2-overexpressing cells is the main reason to hypothesize that FHL2 indeed inhibits adipocyte

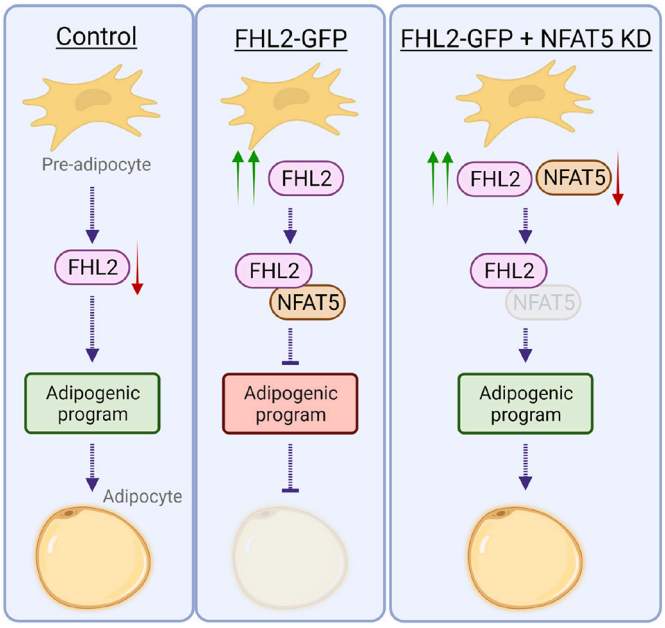

Fig. 6. The FHL2-NFAT5 pathway in early adipocyte differentiation. Summary of the proposed mechanism by which FHL2 overexpression inhibits adipocyte differentiation through complex formation with NFAT5. Downregulation of FHL2 in early adipogenesis is an essential step in the differentiation process. Created with BioRender.com.

differentiation through its interaction with NFAT5. We confirmed the interaction of NFAT5 with FHL2 by co-immunoprecipitation and recovered adipocyte differentiation in overexpressing FHL2 cells by reducing NFAT5 expression. Previously, hypertonicity has been reported as a relevant process in lipid accumulation in 3T3-L1 cells, we may therefore speculate that the FHL2-NFAT5 complex modulates hypertonic stress in pre-adipocytes (45). Another finding that puts forward interesting aspects to be studied further, is our finding that the FHL2 pull-down in 3T3-L1 cells contains eight members of the CNOT complex, which strongly suggests that FHL2 participates in this complex. Given that FHL2 is known to interact with several nuclear receptors, among which ERα, it is of interest to mention that direct interaction of CNOT1 with the nuclear receptors ERα and RXR has been reported (46). Even more relevant for the current study, the CNOT complex is necessary for a correct adipocyte phenotype in mouse adipose tissue, as well as for appropriate differentiation of 3T3-L1 cells (47–49). We wish to propose that it is very likely that the binding of FHL2 with the CNOT complex, with NFAT5, and other factors identified in our pull-down screen, also occurs in other cellular systems undergoing differentiation (16,18). Of note, the interaction between FHL2 and NFAT5, as well as with CNOT-elements has been reported before in the study by Huttlin *et al*, which concerns a protein interaction network study in T293 and HCT116 cells (50). The current study now demonstrates a functional interaction between FHL2 and NFAT5 in adipogenesis, and it will be of interest to assess the relative contribution of this specific protein-protein interaction in other cellular processes.

5. Conclusion

FHL2 is expressed in pre-adipocytes where it refrains the cells from differentiating towards mature adipocytes through its interaction with NFAT5. Our data indicate that the expression of both proteins needs to be reduced to initiate the adipogenic program. Based on the present findings, we can firstly add FHL2 to the list of factors requiring timely regulation of expression to facilitate accurate adipocyte differentiation (3,51,52) and, secondly add adipocytes to the list of cells in which FHL2 plays an important role in differentiation (16,18). Especially in elderly individuals, FHL2 expression in WAT is increased, which may interfere with appropriate adipogenesis and subsequent peripheral fat loss with aging. Finally, whereas FHL2 has been described to promote differentiation of myoblasts and osteoblasts (16,18), we now demonstrated that FHL2 plays the opposite role in pre-adipocytes. Given that these cells are all derived from mesenchymal stem cells, this poses FHL2 at the intersection of these two distinct cellular processes, tilting the balance towards osteoblasts, whereas its downregulation facilitates pre-adipocyte formation (53).

Funding and additional information

This research was supported by grants from the Rembrandt Institute of Cardiovascular Sciences, and Research Institute Cardiovascular Sciences of Amsterdam UMC (C.J.dV.), and by a grant from the European Union's Horizon 2020 Marie Skłodowska-Curie Innovative Training Network, TRAIN (project no. 721532 – E.K.).

Author contribution

M.P. Clemente-Olivo, M. Hernandez-Quiles, E. Kalkhoven, and C.J. M. de Vries conceived the study and experiments. M.P. Clemente-Olivo, M. Hernandez-Quiles, R. Sparrius, M. van der Stoel, and V. Janssen performed the experiments. M.P. Clemente-Olivo, M. Hernandez-Quiles and A. Jongejan performed and analyzed the RNA sequencing experiment. M. Hernandez-Quiles, R. van Es, P. Sobrevals Alcaraz and H. Vos performed and analyzed the mass spectrometry data. M.P. Clemente-Olivo, M. Hernandez-Quiles, E. Kalkhoven, and C.J.M. de Vries wrote the manuscript.

Ethics approval

All animal experiments were approved by the ethics committee of the Amsterdam University Medical Center, The Netherlands, and were performed following European directive 2010/63/EU guidelines (permit number DBC287).

Consent for publication

This study is approved by all authors for publication.

Declaration of Competing Interest

The authors declare they have no conflicts of interest with the contents of this article.

Data availability

The raw and processed RNA-seq data have been deposited in the Gene Expression Omnibus (GEO) database under accession number GSE200920. The mass spectrometry proteomics data have been deposited to the ProteomeXchange Consortium via the PRIDE partner repository with the dataset identifier PXD033974.

Acknowledgments

We thank Dr. Sebastiaan Winkler and members of the Kalkhoven and de Vries laboratories for helpful discussions. Graphical abstract, Fig. 3A and Fig. 6 were created with BioRender.com.

Appendix A. Supplementary data

Supplementary data to this article can be found online at https://doi.org/10.1016/j.cellsig.2023.110587.

References

[1] L.D. Meirelles, A.I. Caplan, N.B. Nardi, In search of the in vivo identity of mesenchymal stem cells, Stem Cells 26 (9) (2008) 2287–2299.
[2] C.E. Lowe, S. O'Rahilly, J.J. Rochford, Adipogenesis at a glance, J. Cell Sci. 124 (16) (2011) 2681–2686.
[3] S.R. Farmer, Transcriptional control of adipocyte formation, Cell Metab. 4 (4) (2006) 263–273.
[4] M. Hernandez-Quiles, M.F. Broekema, E. Kalkhoven, PPARgamma in metabolism, immunity, and cancer: unified and diverse mechanisms of action, Front. Endocrinol. (Lausanne). 12 (2021), 624112.
[5] N. Schaum, B. Lehallier, O. Hahn, R. Palovics, S. Hosseinzadeh, S.E. Lee, et al., Ageing hallmarks exhibit organ-specific temporal signatures, Nature. 583 (7817) (2020) 596–602.
[6] M.Y. Ou, H. Zhang, P.C. Tan, S.B. Zhou, Q.F. Li, Adipose tissue aging: mechanisms and therapeutic implications, Cell Death Dis. 13 (4) (2022) 300.
[7] J.L. Kirkland, T. Tchkonia, T. Pirtskhalava, J. Han, I. Karagiannides, Adipogenesis and aging: does aging make fat go MAD? Exp. Gerontol. 37 (6) (2002) 757–767.
[8] B.M. Schipper, K.G. Marra, W. Zhang, A.D. Donnenberg, J.P. Rubin, Regional anatomic and age effects on cell function of human adipose-derived stem cells, Ann. Plast. Surg. 60 (5) (2008) 538–544.
[9] B. Ahmad, C.J. Serpell, I.L. Fong, E.H. Wong, Molecular mechanisms of adipogenesis: the anti-adipogenic role of AMP-activated protein kinase, Front. Mol. Biosci. (2020) 7.
[10] Y.H. Wang, L. Zhao, C. Smas, H.S. Sul, Pref-1 interacts with fibronectin to inhibit adipocyte differentiation, Mol. Cell. Biol. 30 (14) (2010) 3480–3492.
[11] G.R. Hajer, T.W. van Haeften, F.L. Visseren, Adipose tissue dysfunction in obesity, diabetes, and vascular diseases, Eur. Heart J. 29 (24) (2008) 2959–2971.
[12] M.A. Ambele, P. Dhanraj, R. Giles, M.S. Pepper, Adipogenesis: a complex interplay of multiple molecular determinants and pathways, Int. J. Mol. Sci. 21 (12) (2020) 4283.
[13] J.J. Habibe, M.P. Clemente-Olivo, C.J. de Vries, How (epi)genetic regulation of the LIM-domain protein FHL2 impacts multifactorial disease, Cells. 10 (10) (2021).
[14] M. Johannessen, S. Moller, T. Hansen, U. Moens, M. Van Ghelue, The multifunctional roles of the four-and-a-half-LIM only protein FHL2, Cell. Mol. Life Sci. 63 (3) (2006) 268–284.
[15] P.M. Clemente-Olivo, J.J. Habibe, M. Vos, R. Ottenhoff, A. Jongejan, H. Herrema, et al., Four-and-a-half LIM domain protein 2 (FHL2) deficiency protects mice from diet-induced obesity and high FHL2 expression marks human obesity, Metabol. Clin. Exp. (2021) 121.
[16] J. Brun, O. Fromigue, F.X. Dieudonne, C. Marty, J. Chen, J. Dahan, et al., The LIM-only protein FHL2 controls mesenchymal cell osteogenic differentiation and bone formation through Wnt5a and Wnt10b, Bone. 53 (1) (2013) 6–12.
[17] C.F. Lai, S.T. Bai, B.A. Uthgenannt, L.R. Halstead, P. McLoughlin, B.W. Schafer, et al., Four and half lim protein 2 (FHL2) stimulates osteoblast differentiation, J. Bone Miner. Res. 21 (1) (2006) 17–28.
[18] B. Martin, R. Schneider, S. Janetzky, Z. Waibler, P. Pandur, M. Kuhl, et al., The LIM-only protein FHL2 interacts with beta-catenin and promotes differentiation of mouse myoblasts, J. Cell Biol. 159 (1) (2002) 113–122.
[19] S.J. Kim, T. Kim, H.N. Choi, E.J. Cho, J.B. Park, B.H. Jeon, et al., TonEBP suppresses adipocyte differentiation via modulation of early signaling in 3T3-L1 cells, Korean J. Physiol. Pharmacol. 20 (6) (2016) 649–655.
[20] J.H. Lee, H.H. Lee, B.J. Ye, W. Lee-Kwon, S.Y. Choi, H.M. Kwon, TonEBP suppresses adipogenesis and insulin sensitivity by blocking epigenetic transition of PPARgamma2, Sci. Rep. 5 (2015) 10937.
[21] M. Rakhshandehroo, S.M. Gijzel, R. Siersbaek, M.F. Broekema, C. de Haar, H. S. Schipper, et al., CD1d-mediated presentation of endogenous lipid antigens by adipocytes requires microsomal triglyceride transfer protein, J. Biol. Chem. 289 (32) (2014) 22128–22139.
[22] K. Kurakula, M. Vos, I.O. Rubio, G. Marinkovic, R. Buettner, L.C. Heukamp, et al., The LIM-only protein FHL2 reduces vascular lesion formation involving inhibition of proliferation and migration of smooth muscle cells, PLoS One 9 (4) (2014).
[23] J.M. Ruijter, C. Ramakers, W.M.H. Hoogaars, Y. Karlen, O. Bakker, M.J.B. van den Hoff, et al., Amplification efficiency: linking baseline and bias in the analysis of quantitative PCR data, Nucleic Acids Res. 37 (6) (2009).
[24] D. Kim, B. Langmead, S.L. Salzberg, HISAT: a fast spliced aligner with low memory requirements, Nat. Methods 12 (4) (2015) 357–360.
[25] M.D. Robinson, D.J. McCarthy, G.K. Smyth, edgeR: a Bioconductor package for differential expression analysis of digital gene expression data, Bioinformatics. 26 (1) (2010) 139–140.
[26] A.M. Bolger, M. Lohse, B. Usadel, Trimmomatic: a flexible trimmer for Illumina sequence data, Bioinformatics. 30 (15) (2014) 2114–2120.
[27] D. Wu, G.K. Smyth, Camera: a competitive gene set test accounting for inter-gene correlation, Nucleic Acids Res. 40 (17) (2012), e133.
[28] K. Kurakula, E. van der Wal, D. Geerts, C.M. van Tiel, C.J.M. de Vries, FHL2 protein is a novel co-repressor of nuclear receptor Nur77, J. Biol. Chem. 286 (52) (2011) 44336–44343.
[29] H. Green, M. Meuth, An established pre-adipose cell line and its differentiation in culture, Cell. 3 (2) (1974) 127–133.
[30] F.J. Ruiz-Ojeda, A.I. Ruperez, C. Gomez-Llorente, A. Gil, C.M. Aguilera, Cell models and their application for studying adipogenic differentiation in relation to obesity: a review, Int. J. Mol. Sci. 17 (7) (2016).
[31] S. Ruijtenberg, S. van den Heuvel, Coordinating cell proliferation and differentiation: antagonism between cell cycle regulators and cell type-specific gene expression, Cell Cycle 15 (2) (2016) 196–212.
[32] C. Jiang, J. Sun, Y. Dai, P. Cao, L. Zhang, S. Peng, et al., HIF-1A and C/EBPs transcriptionally regulate adipogenic differentiation of bone marrow-derived MSCs in hypoxia, Stem Cell Res Ther 6 (2015) 21.
[33] S.N. Li, J.F. Wu, TGF-beta/SMAD signaling regulation of mesenchymal stem cells in adipocyte commitment, Stem Cell Res Ther 11 (1) (2020) 41.
[34] M.K. Tran, K. Kurakula, D.S. Koenis, C.J.M. de Vries, Protein-protein interactions of the LIM-only protein FHL2 and functional implication of the interactions relevant in cardiovascular disease, Bba-Mol. Cell. Res. 1863 (2) (2016) 219–228.
[35] M. Hernandez-Quiles, R. Baak, A. Borgman, S. den Haan, P. Sobrevals Alcaraz, R. van Es, et al., Comprehensive profiling of mammalian tribbles interactomes implicates TRIB3 in gene repression, Cancers (Basel). 13 (24) (2021).
[36] H.H. Lee, S.M. An, B.J. Ye, J.H. Lee, E.J. Yoo, G.W. Jeong, et al., TonEBP/NFAT5 promotes obesity and insulin resistance by epigenetic suppression of white adipose tissue beiging, Nat. Commun. 10 (1) (2019) 3536.
[37] N. Chalabi Hagkarim, R.J. Grand, The regulatory properties of the Ccr4-not complex, Cells. 9 (11) (2020).
[38] M.A. Collart, O.O. Panasenko, The Ccr4-not complex: architecture and structural insights, Subcell. Biochem. 83 (2017) 349–379.
[39] G.P. Mognol, F.R.G. Carneiro, B.K. Robbs, D.V. Faget, J.P.B. Viola, Cell cycle and apoptosis regulation by NFAT transcription factors: new roles for an old player, Cell Death Dis. (2016) 7.
[40] W.P. Sun, Z.J. Yu, S.M. Yang, C.Y. Jiang, Y.B. Kou, L.Z. Xiao, et al., A transcriptomic analysis reveals novel patterns of gene expression during 3T3-L1 adipocyte differentiation, Front. Mol. Biosci. (2020) 7.
[41] Y.C. Fu, N.L. Luo, R.L. Klein, W.T. Garvey, Adiponectin promotes adipocyte differentiation, insulin sensitivity, and lipid accumulation, J. Lipid Res. 46 (7) (2005) 1369–1379.
[42] V. Christiaens, M. Van Hul, H.R. Lijnen, I. Scroyen, CD36 promotes adipocyte differentiation and adipogenesis, Bba-Gen Subjects. 1820 (7) (2012) 949–956.
[43] S.D. Lee, S.Y. Choi, S.W. Lim, S.T. Lamitina, S.N. Ho, W.Y. Go, et al., TonEBP stimulates multiple cellular pathways for adaptation to hypertonic stress: organic osmolyte-dependent and -independent pathways, Am. J. Physiol. Ren. Physiol. 300 (3) (2011) F707–F715.
[44] N. Lee, D. Kim, W.U. Kim, Role of NFAT5 in the immune system and pathogenesis of autoimmune diseases, Front. Immunol. 10 (2019).
[45] E.E. Ha, R.C. Bauer, Emerging roles for adipose tissue in cardiovascular disease, Arterioscl. Throm. Vas. 38 (8) (2018). E137-E44.
[46] G.S. Winkler, K.W. Mulder, V.J. Bardwell, E. Kalkhoven, H.T. Timmers, Human Ccr4-not complex is a ligand-dependent repressor of nuclear receptor-mediated transcription, EMBO J. 25 (13) (2006) 3089–3099.
[47] X. Li, M. Morita, C. Kikuguchi, A. Takahashi, T. Suzuki, T. Yamamoto, Adipocyte-specific disruption of mouse Cnot3 causes lipodystrophy, FEBS Lett. 591 (2) (2017) 358–368.
[48] A. Takahashi, S. Takaoka, S. Kobori, T. Yamaguchi, S. Ferwati, K. Kuba, et al., The CCR4-NOT deadenylase complex maintains adipocyte identity, Int. J. Mol. Sci. 20 (21) (2019).
[49] E.J. Sohn, D.B. Jung, J. Lee, S.W. Yoon, G.H. Won, H.S. Ko, et al., CCR4-NOT2 promotes the differentiation and lipogenesis of 3T3-L1 adipocytes via upregulation of PPARx03B3;, CEBPalpha and inhibition of P-GSK3alpha/beta and beta-catenin, Cell. Physiol. Biochem. 37 (5) (2015) 1881–1889.
[50] E.L. Huttlin, R.J. Bruckner, J. Navarrete-Perea, J.R. Cannon, K. Baltier, F. Gebreab, et al., Dual proteome-scale networks reveal cell-specific remodeling of the human interactome, Cell. 184 (11) (2021), 3022-+.
[51] M. Audano, S. Pedretti, D. Caruso, M. Crestani, E. De Fabiani, N. Mitro, Regulatory mechanisms of the early phase of white adipocyte differentiation: an overview, Cell. Mol. Life Sci. 79 (3) (2022) 139.
[52] E. Mueller, Understanding the variegation of fat: novel regulators of adipocyte differentiation and fat tissue biology, Biochim. Biophys. Acta 1842 (3) (2014) 352–357.
[53] A.W. James, Review of signaling pathways governing MSC osteogenic and Adipogenic differentiation, Scientifica. 2013 (2013).